

# A two-carrier scheme: evading the 3dB quantum penalty of heterodyne readout in gravitational-wave detectors

Teng Zhang<sup>1</sup>, Philip Jones<sup>1</sup>, Haixing Miao<sup>1</sup>, Denis Martynov<sup>1</sup>, Andreas Freise<sup>1,2,3</sup>, and Stefan W. Ballmer<sup>4</sup>

<sup>1</sup>*School of Physics and Astronomy, and Institute of Gravitational Wave Astronomy, University of Birmingham, Edgbaston, Birmingham B15 2TT, United Kingdom*

<sup>2</sup>*Department of Physics and Astronomy, VU Amsterdam, De Boelelaan 1081, 1081, HV, Amsterdam, The Netherlands*

<sup>3</sup>*Nikhef, Science Park 105, 1098, XG Amsterdam, The Netherlands and*

<sup>4</sup>*Syracuse University, Syracuse, NY 13244, USA*

Precision measurements using traditional heterodyne readout suffer a 3dB quantum noise penalty compared with homodyne readout. The extra noise is caused by the quantum fluctuations in the image vacuum. We propose a two-carrier gravitational-wave detector design that evades the 3dB quantum penalty of heterodyne readout. Such a heterodyne readout scheme can reduce technical complexity and technical noise couplings compared to homodyne readout. We further propose a new way to realise frequency-dependent squeezing utilising two-mode squeezing in our scheme. It naturally achieves more precise audio frequency signal measurements with radio frequency squeezing, which avoids the classical noise at audio frequency. In addition, the detector is compatible with other quantum nondemolition techniques.

*Introduction* — Since 2015, laser interferometric gravitational-wave detectors have made a series of direct observations of gravitational waves from mergers of binary black holes and neutron stars [1–3]. They have opened a new observational window into the universe and provided significant new inputs to many scientific fields. These detectors are dual-recycled Fabry–Perot Michelson interferometers. In the interferometer, a laser field is pumped from the symmetric port, enhanced in the power recycling cavity and then circulated in the two Fabry–Perot arm cavities. This laser is called the carrier laser, which senses the motion of the test masses induced by the gravitational waves. When the interferometer operates at the dark fringe, the carrier will return to the symmetric port, while the signal sidebands encoding the differential motion of the two arm cavities enter into the anti-symmetric port. The signal-recycling cavity plays the role of circulating the signal sidebands, which shapes the frequency-dependent response of the interferometer [4–6]. To translate the electromagnetic sidebands into a measurable electrical signal, an optical readout scheme is required, which is also fundamental for determining the sensitivity of the detector [7].

Heterodyne readout is widely implemented in precision measurements, for example, for the stabilisation of laser frequencies and optical cavities (also known as the Pound-Drever-Hall technique [8, 9]) and for quantum squeezing characterisation due to its natural immunity to the low-frequency classical noise [10–14]. Compared with homodyne readout, heterodyne readout suffers from a 3dB noise penalty as the scheme picks up the vacuum fields above and below the local oscillator. The additional field that does not coincide with the signal is called the image vacuum [15–18]. The additional noise penalty is a direct and necessary consequence of the Heisenberg uncertainty principle when all quadratures are allowed to be

measured simultaneously [19]. In the first-generation of gravitational wave detectors, *e.g.* LIGO [20], Virgo [21], TAMA [22], GEO600 [23], a heterodyne readout with two balanced radio frequency (RF) sidebands was used [24], reducing the factor of 2 (3dB) quantum penalty to a factor of 1.5. In this scheme, the fields which are twice the modulation frequency away from the central carrier also

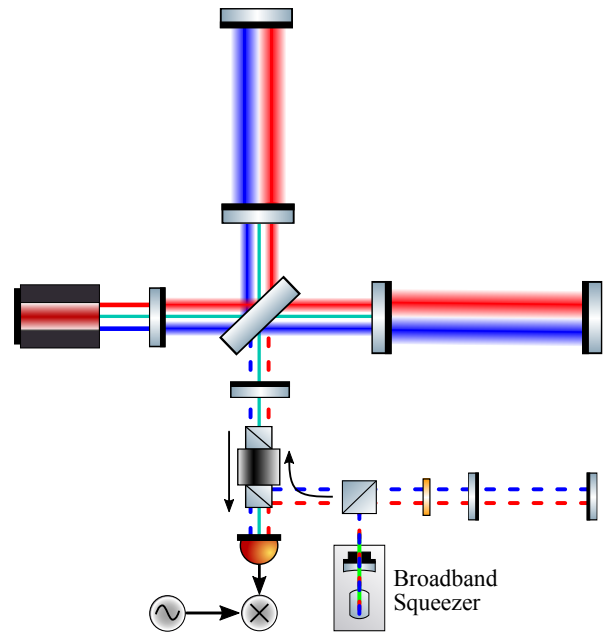


FIG. 1. Schematic of the two-carrier gravitational-wave detector with heterodyne readout. The red, blue and cyan lasers correspond to the carriers at  $\omega_1$ ,  $\omega_2$  and the local oscillator at  $\omega_L = (\omega_1 + \omega_2)/2$ , respectively. The three beams are spatially overlapped in the detector. The broadband squeezer has a bandwidth larger than  $\omega_m + \Omega$ , but without the need for squeezing at audio frequencies.

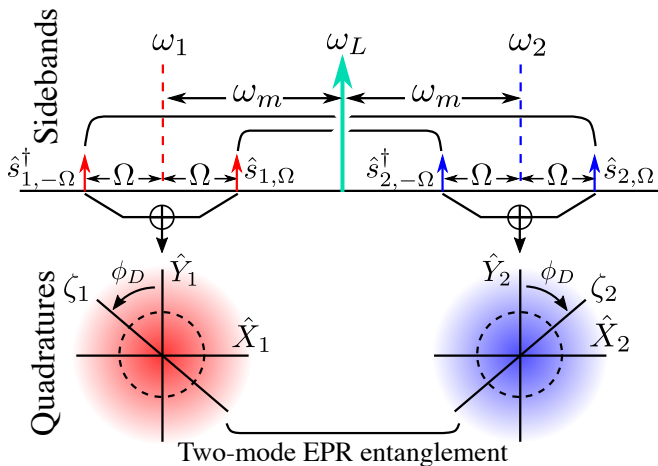


FIG. 2. Two-carrier heterodyne readout with two-mode squeezing: sideband picture (top) and quadrature picture (bottom). The two carriers are at frequencies  $\omega_1$  and  $\omega_2$ . The single local oscillator field (or "single sideband") is in the middle at  $\omega_L = (\omega_1 + \omega_2)/2$ . The squeezer is pumped at  $2\omega_L$ , entangling sideband pairs symmetric around the local oscillator field at  $\omega_L$ . This leads to a two-mode EPR entanglement between quadratures on  $\zeta_1$  and  $\zeta_2$ .  $\Omega$  is the frequency of the audio signal sideband and  $\omega_m$  is the separation between the local oscillator and each carrier.

couple to the readout channel [19]. The quantum fluctuations from these image vacuum fields also contribute to the total quantum noise [17]. In subsequent detector upgrades the readout scheme was switched to DC readout [24, 25], a variant of homodyne readout. The local oscillator in the DC readout is derived by slightly detuning the arm cavities, which offsets the interferometer from a perfect dark fringe. DC readout has the advantage of a straightforward implementation without needing an external local oscillator. However, the dark-fringe offset induces extra couplings of technical noises and is not ideal for future-generation gravitational wave detectors [26]. A balanced homodyne readout can eliminate the dark fringe offset by introducing a spatially separated local oscillator [7]. This requires auxiliary optics on the local oscillator path and additional output optical mode cleaner, which introduces extra complexities [27]. Meanwhile, heterodyne readout is still used in current detectors for the stabilisation of auxiliary degrees of freedom, such as the lengths of the two recycling cavities [28, 29].

Is there a way to evade the fundamental quantum noise penalty with heterodyne readout? It was found that the noise penalty of heterodyne readout could be evaded if the image vacuum fields can be excited to contain coherent signal flux [17, 30]. Inspired by this finding, we propose a new gravitational wave detector design that includes two carriers at  $\omega_1$  and  $\omega_2$  with a beam at  $\omega_L = (\omega_1 + \omega_2)/2$  serving as the heterodyne local oscillator. The three beams are evenly separated by an

RF frequency  $\omega_m$ . They have the same spatial mode in the detector. The schematic of the design is shown in Fig. 1. The two carriers resonant and the local oscillator anti-resonant in the arm cavities. The local oscillator resonates in recycling cavities. This new design with heterodyne readout will lead to identical quantum-limited sensitivity performance as with homodyne readout and the same total arm power, *i.e.* the sum of the power of the two carriers circulating in the arm equals to the arm cavity power in the single-carrier detector with homodyne readout.

Another highlight of the two-carrier detector with heterodyne readout is the simplicity of generating and applying quantum squeezing. Most gravitational-wave signals from compact binary system detected by ground-based detectors are within the audio band, from several hertz to several kilohertz. However, at audio frequencies, excess noises are significant due to the parasitic interferences from back-scattered light [31, 32] and noise coupling from control beams [33–38]. Good squeezing is easier to produce and observe at high frequencies in the MHz range [33, 37, 39–42], where the classical noise of the laser is negligible. We will show that instead of audio-band squeezing [43, 44], high-frequency squeezing in a broadband two-mode quantum state is sufficient in our configuration. Our scheme naturally allows measurement of low-frequency signals with high-frequency squeezing [45, 46].

*Heterodyne readout and two-mode squeezing* — As shown in Fig. 1 and 2, in a single sideband heterodyne readout, two sideband modes,  $\hat{s}_{1,\pm\Omega}$ ,  $\hat{s}_{2,\pm\Omega}$  around frequencies  $\omega_1$  and  $\omega_2$  are measured. The eventual output photocurrent of the heterodyne readout can be derived as

$$I = e^{i(\phi_L - \phi_D)} \hat{s}_{1,\pm\Omega}^\dagger + e^{i(\phi_L + \phi_D)} \hat{s}_{2,\pm\Omega}^\dagger + h.c., \quad (1)$$

where  $\phi_L$  is the local oscillator phase and is assumed to be  $\pi/2$  in this work,  $\phi_D$  is the demodulation phase, the local oscillator amplitude is assumed to be 1 and *h.c.* denotes the Hermitian conjugate. In the two-photon formalism [47, 48], the photocurrent is proportional to the combined quadrature [49]

$$\hat{Q}_\zeta = \mathbf{H}_\zeta \cdot [\hat{X}_1 \ \hat{Y}_1 \ \hat{X}_2 \ \hat{Y}_2]^\text{T}, \quad (2)$$

with  $\mathbf{H}_\zeta \equiv [\cos \zeta_1, \sin \zeta_1, \cos \zeta_2, \sin \zeta_2]$ . Here  $\hat{X}_j, \hat{Y}_j$  ( $j = 1, 2$ ) represent the amplitude and phase quadrature of the sidebands  $\hat{s}_{1,\pm\Omega}$  and  $\hat{s}_{2,\pm\Omega}$ , respectively;  $\zeta_j$  defines the measurement quadrature,

$$\zeta_1 = \phi_L - \phi_D, \zeta_2 = \phi_L + \phi_D \quad (3)$$

We normalise the shot noise spectral density for the vacuum state to be 1. In the two-mode quantum state,  $\hat{s}_1$  and  $\hat{s}_2$  are correlated [10, 38, 49, 50], of which the corre-

lation is quantified by the covariance matrix,

$$\mathbb{V} = \begin{bmatrix} \alpha & 0 & \beta & 0 \\ 0 & \alpha & 0 & -\beta \\ \beta & 0 & \alpha & 0 \\ 0 & -\beta & 0 & \alpha \end{bmatrix}, \quad (4)$$

where  $\alpha = \cosh 2r$ ,  $\beta = \sinh 2r$  and  $r$  is the phase squeezing factor. The spectral density of the combined quadrature  $\hat{Q}_\zeta$  in Eq. (2) is given by

$$\mathbf{H}_\zeta \mathbb{V} \mathbf{H}_\zeta^T = 2\alpha - 2\beta = 2e^{-2r}, \quad (5)$$

which is a natural result of the EPR entanglement between quadratures of the two modes [12, 51–53], as illustrated in Fig. 2. As we can observe, to measure the sidebands at  $\Omega$  with higher accuracy beyond the shot noise limit, squeezing only at high frequencies—*i.e.*  $\omega_m$  away from half of the pumping frequency—is required. This means that although we need a broadband squeezer with a central frequency at  $\omega_L$  and bandwidth larger than  $\omega_m + \Omega$ , good squeezing around  $\omega_L$  is not required. In a conventional single carrier scheme, in which only one of the two modes takes signal, the noise to signal ratio is  $2e^{-2r}$ , where the signal part is normalised to be 1. The factor of 2 here corresponds to the well-known 3dB quantum penalty. In the two carrier scheme, the same total power is divided into two carriers equally, and the noise to signal ratio becomes  $2e^{-2r}/(\sqrt{2}/2 + \sqrt{2}/2)^2 = e^{-2r}$ , which demonstrates the evasion of the 3dB penalty.

*Quantum noise of the detector* — So far, we have been focusing on shot noise. Inside the interferometer, the two sideband modes interact with the test mass through the radiation pressure force by beating with the two carriers, which also introduces radiation pressure noise. When the interferometer is tuned with equal power in the two carriers, the opto-mechanical factors describing the interaction of the modes with the test mass mirrors and their cross correlation are identical. They are equal to half of the opto-mechanical factor  $\mathcal{K}$  defined in Ref. [55]. Note that here, because  $\omega_m$  is much smaller than  $\omega_j$ , we neglect the effect of the difference in the wavelength of two carriers. The input-output transfer matrix  $\mathbb{T}$  for the quadratures of these two modes and their response vector  $\mathbf{R}$  of the interferometer to the gravitational wave strain can be derived as

$$\mathbb{T} = e^{2i\beta} \begin{bmatrix} 1 & 0 & 0 & 0 \\ -\mathcal{K}/2 & 1 & -\mathcal{K}/2 & 0 \\ 0 & 0 & 1 & 0 \\ -\mathcal{K}/2 & 0 & -\mathcal{K}/2 & 1 \end{bmatrix}, \quad \mathbf{R} = \frac{e^{i\beta}}{h_{\text{SQL}}} \begin{bmatrix} 0 \\ \sqrt{\mathcal{K}} \\ 0 \\ \sqrt{\mathcal{K}} \end{bmatrix}. \quad (6)$$

Here  $\beta = \text{atan}(\Omega/\gamma)$  is the phase of the sidebands at frequency  $\Omega$  acquired by reflection from the interferometer with an effective bandwidth  $\gamma$ . The opto-mechanical factor is

$$\mathcal{K} = \frac{16\omega_0 P \gamma}{mcL\Omega^2(\gamma^2 + \Omega^2)}, \quad (7)$$

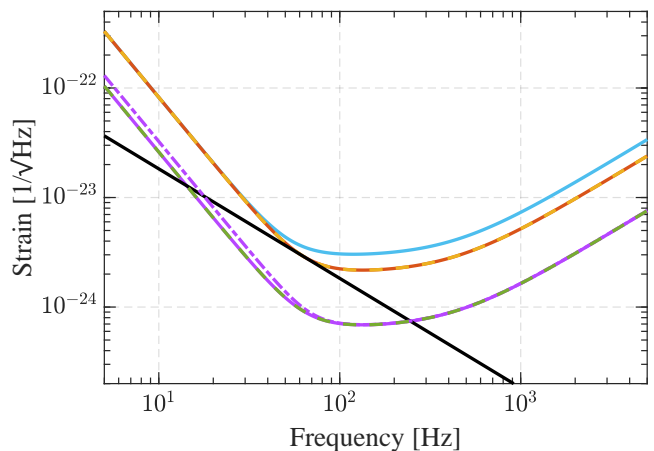


FIG. 3. Quantum-limited sensitivity of different configurations. The blue curve corresponds to the case of a single-carrier detector with heterodyne readout. The orange curve corresponds to the two-carrier detector, which perfectly overlaps with the dashed yellow curve for homodyne readout. The solid purple curve is the sensitivity of the two-carrier detector with 10dB squeezing, which perfectly overlaps with the dashed green curve for homodyne readout with the same squeezing level. The dot-dashed purple curve corresponds to a 15% power imbalance between the two carriers while the total power stays constant. The black curve is the Standard Quantum Limit. The detector and filter cavity parameters used in the two-carrier detector are the same as those of Advanced LIGO [6] and Advanced LIGO upgrade [54].

where  $m$  is the mirror mass, and  $P$  is the total circulating power in the arm cavity. The Standard Quantum Limit of the detector in strain is  $h_{\text{SQL}} = \sqrt{8\hbar/(m\Omega^2 L^2)}$ .

The low-frequency radiation pressure noise can be improved by using frequency-dependent squeezing [55]. Similarly to the single-carrier detector, we only need one filter cavity for the two-carrier detector, as long as  $2\omega_m$  is an integer multiple of the free spectral range of the filter cavity. The filter cavity provides a frequency dependent quadrature rotation  $\theta_1, \theta_2$  for the two modes, which can be described by [56]

$$\mathbb{P}_\theta = \begin{bmatrix} \cos \theta_1 & -\sin \theta_1 & 0 & 0 \\ \sin \theta_1 & \cos \theta_1 & 0 & 0 \\ 0 & 0 & \cos \theta_2 & -\sin \theta_2 \\ 0 & 0 & \sin \theta_2 & \cos \theta_2 \end{bmatrix}. \quad (8)$$

The quantum noise spectral density of heterodyne readout, normalised to the strain response, is given by

$$S_{hh} = h_{\text{SQL}}^2 \frac{\mathbf{H}_\zeta \mathbb{T} \mathbb{P}_\theta \mathbb{V} \mathbb{P}_\theta^T \mathbb{T}^\dagger \mathbf{H}_\zeta^T}{|\mathbf{H}_\zeta \mathbf{R}|^2}. \quad (9)$$

When the frequency-dependent rotation angle satisfies

$$\theta_1 = \theta_2 = \text{atan } \mathcal{K}, \quad (10)$$

the noise spectrum reaches the minimal value

$$S_{hh}^{\text{min}} = \frac{h_{\text{SQL}}^2}{2} \frac{\mathcal{K}^2 + 1}{\mathcal{K}} e^{-2r}. \quad (11)$$

According to Eq. 10, the required frequency dependent rotation angle is the same as that in the single-carrier detector [55]. Thus, the filter cavity parameters can be kept the same as in the single carrier scheme. In Fig. 3, we plot the noise spectral densities for different configurations as a comparison. The two-carrier detector with heterodyne readout gives identical sensitivity to that of Advanced LIGO with homodyne readout. The figure also shows that the scheme is robust against a power imbalance between the two carriers. A rather large 15% power imbalance between the two carriers under 10dB frequency-dependent squeezing only results in a 20% degradation in sensitivity at low frequencies. Here the total power remains the same. The reason for the sensitivity degradation mainly comes from the imbalanced combination of two entangled modes when there is injection of two-mode squeezing. It only appears in lower frequencies due to the imbalanced radiation pressure effect. The effect of 15% signal imbalance is negligible, leading to only a 0.57% sensitivity degradation in high frequencies.

*Criteria for macroscopic lengths* — One important difference between our proposed scheme and the single-carrier detector is that the lengths between core optics need to be carefully set to defined absolute values to guarantee co-resonance of the respective optical fields. This introduces new requirements on the macroscopic lengths, in addition to the usual requirements for controlling the microscopic position of the optics via feedback. We anticipate this co-resonance requirement to be relatively easy to achieve, as the current lock acquisition system already permits selecting a specific fringe.

To keep the carriers resonant and the local oscillator beam anti-resonant in the arm cavities,  $2\omega_m$  shall be an odd multiple of the free spectral range of the arm cavity,  $c/(2L)$ . Another consideration is on the coupling between the symmetric and anti-symmetric ports for both the carriers and the local oscillator. Taking the local oscillator field as DC by convention ( $\omega_L = 0$ ,  $\omega_1 = -\omega_m$ ,  $\omega_2 = \omega_m$ ), and locking the central Michelson on its bright fringe, we can treat the central Michelson as an effective mirror with amplitude transmissivity

$$r_{\text{MI}} = ir_a \sin \frac{\omega \Delta l}{c}, \quad t_{\text{MI}} = r_a \cos \frac{\omega \Delta l}{c}, \quad (12)$$

where  $\omega$  is the RF sideband frequency,  $\Delta l$  is the Schnupp asymmetry [29], and  $r_a$  is the amplitude reflectivity of arm cavities. For the local oscillator anti-resonating in the arm cavities,  $r_a = -1$ , and  $\omega = \omega_L = 0$ . For the carriers we have  $r_a = 1$ , as well as  $\omega = \omega_1 = -\omega_m$  and  $\omega = \omega_2 = +\omega_m$  respectively. To keep the carriers on the Michelson dark fringe we need to have  $\omega_m \Delta l / c = \pi/2$ . The macroscopic round-trip length of the signal recycling cavity and power recycling cavity should be tuned to satisfy the following conditions: in the signal recycling cavity, the signal (carrier) modes are anti-resonant, while the local oscillator beam is resonant; in the power recy-

cling cavity, all three beams are on resonance. At the input port, the two carriers require a  $\pi/2$  phase difference relative to the local oscillator, which is the same phase relationship as sidebands generated through phase modulation. In Advanced LIGO,  $\omega_m$  is around 45 MHz, so  $\Delta l$  needs to be around 1.67 m. Given the Advanced LIGO power and signal recycling mirror transmissivities of 0.03 and 0.325, the effective power transmissivity of the local oscillator field from the symmetric port to the anti-symmetric port is around 25%. Finally, to implement frequency-dependent squeezing, according to Eq. (10) the required rotations for the two modes are identical to each other, as well as that in the single-carrier detector with homodyne readout. To use one filter cavity for two modes, we need  $2\omega_m$  to be an integer multiple of the free spectral range of the filter cavity, as mentioned earlier.

*Conclusions and Discussions* — We have shown that the proposed two-carrier gravitational wave detector with heterodyne readout leads to a quantum-limited sensitivity identical to that of homodyne readout. To implement frequency dependent squeezing, only one filter cavity is required, which is the same as the single-carrier detector with homodyne readout. Furthermore, the two-carrier detector also provides advantages for mitigating other noise contributions: (1) it enables squeezing enhanced measurements in the audio-band and below with high-frequency squeezing, which is immune to the low-frequency classical noise; (2) it allows us to operate the interferometer on the dark fringe without an additional local oscillator path and output mode cleaners that are essential to the balanced homodyne readout scheme, in which two mode cleaners are required [49]. If the higher optical modes at the dark port cannot be suppressed by the interferometer itself, one output mode cleaner of which the free spectral range equals to  $\omega_m$  is sufficient. Compared with the single-carrier detector, there is added complexity related to the creation of two carriers on the input laser side. We also need a detailed study of the modulation scheme and classical noise couplings, *e.g.* laser frequency noise coupling due to a larger Schnupp asymmetry, in order to eventually implement it.

As an outlook, we also want to highlight that the two-carrier detector is also compatible with general quantum nondemolition (QND) measurement schemes [57, 58], in contrast to conventional heterodyne readout [19]. For example, similar to the implementation of frequency dependent squeezing, we can add a filter cavity at the output to realise frequency-dependent readout for back action evasion [55]. The resulting optimal sensitivity is

$$S_{hh}^{\text{opt}} = \frac{h_{\text{SQL}}^2}{2} \frac{1}{\mathcal{K}} e^{-2r}. \quad (13)$$

This saturates the fundamental quantum limit or the quantum Cramér-Rao bound [59–62].

*Acknowledgements* — We thank the support from simulation software, *Finesse*. T. Z., P.J., H. M., D. M. and A. F. acknowledge the support of the Institute for Gravitational Wave Astronomy at University of Birmingham. A. F. has been supported by a Royal Society Wolfson Fellowship which is jointly funded by the Royal Society and the Wolfson Foundation. H. M. is supported by UK STFC Ernest Rutherford Fellowship (Grant No. ST/M005844/11). S.W.B. acknowledges the supported by the National Science Foundation award PHY-1912536. This document was assigned the LIGO document control number LIGO-P2000260.

- 
- [1] B. Abbott, R. Abbott, T. Abbott, M. Abernathy, F. Acernese, K. Ackley, C. Adams, T. Adams, P. Addesso, R. Adhikari, et al. (LIGO Scientific Collaboration and Virgo Collaboration), Observation of gravitational waves from a binary black hole merger, *Phys. Rev. Lett.* **116**, 061102 (2016).
- [2] B. Abbott, R. Abbott, T. Abbott, M. Abernathy, F. Acernese, K. Ackley, C. Adams, T. Adams, P. Addesso, R. Adhikari, et al. (LIGO Scientific Collaboration and Virgo Collaboration), Gw170817: Observation of gravitational waves from a binary neutron star inspiral, *Phys. Rev. Lett.* **119**, 161101 (2017).
- [3] B. Abbott, R. Abbott, T. Abbott, M. Abernathy, F. Acernese, K. Ackley, C. Adams, T. Adams, P. Addesso, R. Adhikari, et al. (LIGO Scientific Collaboration and Virgo Collaboration), Gwtc-1: A gravitational-wave transient catalog of compact binary mergers observed by ligo and virgo during the first and second observing runs, *Phys. Rev. X* **9**, 031040 (2019).
- [4] A. Buonanno and Y. Chen, Signal recycled laser-interferometer gravitational-wave detectors as optical springs, *Phys. Rev. D* **65**, 042001 (2002).
- [5] A. Buonanno and Y. Chen, Scaling law in signal recycled laser-interferometer gravitational-wave detectors, *Phys. Rev. D* **67**, 062002 (2003).
- [6] J. Aasi, B. P. Abbott, R. Abbott, T. Abbott, M. R. Abernathy, K. Ackley, C. Adams, T. Adams, P. Addesso, R. X. Adhikari, and L. S. Collaboration, Advanced LIGO, *Classical and Quantum Gravity* **32**, 074001 (2015).
- [7] P. Fritschel, M. Evans, and V. Frolov, Balanced homodyne readout for quantum limited gravitational wave detectors, *Opt. Express* **22**, 4224 (2014).
- [8] R. W. P. Drever, J. L. Hall, F. V. Kowalski, J. Hough, G. M. Ford, A. J. Munley, and H. Ward, Laser phase and frequency stabilization using an optical resonator, *Applied Physics B* **31**, 97 (1983).
- [9] E. D. Black, An introduction to pound-drever-hall laser frequency stabilization, *American Journal of Physics* **69**, 79 (2001).
- [10] J. Gea-Banacloche and G. Leuchs, Squeezed states for interferometric gravitational-wave detectors, *Journal of Modern Optics* **34**, 793 (1987).
- [11] V. Chickarmane, S. V. Dhurandhar, T. C. Ralph, M. Gray, H.-A. Bachor, and D. E. McClelland, Squeezed light in a frontal-phase-modulated signal-recycled interferometer, *Phys. Rev. A* **57**, 3898 (1998).
- [12] A. M. Marino, J. C. R. Stroud, V. Wong, R. S. Bennink, and R. W. Boyd, Bichromatic local oscillator for detection of two-mode squeezed states of light, *J. Opt. Soc. Am. B* **24**, 335 (2007).
- [13] W. Li, X. Yu, and J. Zhang, Measurement of the squeezed vacuum state by a bichromatic local oscillator, *Opt. Lett.* **40**, 5299 (2015).
- [14] S. Feng, D. He, and B. Xie, Quantum theory of phase-sensitive heterodyne detection, *J. Opt. Soc. Am. B* **33**, 1365 (2016).
- [15] S. D. Personick, B.s.t.j. brief: An image band interpretation of optical heterodyne noise, *The Bell System Technical Journal* **50**, 213 (1971).
- [16] H. P. Yuen and V. W. S. Chan, Noise in homodyne and heterodyne detection, *Opt. Lett.* **8**, 177 (1983).
- [17] M. Collett, R. Loudon, and C. Gardiner, Quantum theory of optical homodyne and heterodyne detection, *Journal of Modern Optics* **34**, 881 (1987).
- [18] C. M. Caves and P. D. Drummond, Quantum limits on bosonic communication rates, *Rev. Mod. Phys.* **66**, 481 (1994).
- [19] A. Buonanno, Y. Chen, and N. Mavalvala, Quantum noise in laser-interferometer gravitational-wave detectors with a heterodyne readout scheme, *Phys. Rev. D* **67**, 122005 (2003).
- [20] D. Sigg and the LIGO Scientific Collaboration, Status of the LIGO detectors, *Classical and Quantum Gravity* **25**, 114041 (2008).
- [21] F. Acernese, M. Alshourbagy, P. Amico, F. Antonucci, S. Aoudia, P. Astone, S. Avino, L. Baggio, et al., Status of virgo, *Classical and Quantum Gravity* **25**, 114045 (2008).
- [22] R. Takahashi and the TAMA Collaboration, Status of TAMA300, *Classical and Quantum Gravity* **21**, S403 (2004).
- [23] H. Grote and the LIGO Scientific Collaboration, The status of GEO 600, *Classical and Quantum Gravity* **25**, 114043 (2008).
- [24] S. Hild, H. Grote, J. Degallaix, S. Chelkowski, K. Danzmann, A. Freise, M. Hewitson, J. Hough, H. Lück, M. Prijatelj, K. A. Strain, J. R. Smith, and B. Willke, DC-readout of a signal-recycled gravitational wave detector, *Classical and Quantum Gravity* **26**, 055012 (2009).
- [25] T. T. Fricke, N. D. Smith-Lefebvre, R. Abbott, R. Adhikari, K. L. Dooley, M. Evans, P. Fritschel, V. V. Frolov, K. Kawabe, J. S. Kissel, B. J. J. Slagmolen, and S. J. Waldman, DC readout experiment in enhanced LIGO, *Classical and Quantum Gravity* **29**, 065005 (2012).
- [26] H. Yu, D. Martynov, S. Vitale, M. Evans, D. Shoemaker, B. Barr, G. Hammond, S. Hild, J. Hough, S. Huttner, S. Rowan, B. Sorazu, L. Carbone, A. Freise, C. Mow-Lowry, K. L. Dooley, P. Fulda, H. Grote, and D. Sigg, Prospects for detecting gravitational waves at 5 hz with ground-based detectors, *Phys. Rev. Lett.* **120**, 141102 (2018).
- [27] S. Steinlechner, B. W. Barr, A. S. Bell, S. L. Danilishin, A. Gläflke, C. Gräf, J.-S. Hennig, E. A. Houston, S. H. Huttner, S. S. Leavey, D. Pascucci, B. Sorazu, A. Spencer, K. A. Strain, J. Wright, and S. Hild, Local-oscillator noise coupling in balanced homodyne readout for advanced gravitational wave detectors, *Phys. Rev. D* **92**, 072009 (2015).
- [28] M. A. Arain and G. Mueller, Design of the advanced ligo recycling cavities, *Optics Express* **16**, 10018 (2008).

- [29] K. Izumi and D. Sigg, Advanced LIGO: length sensing and control in a dual recycled interferometric gravitational wave antenna, *Classical and Quantum Gravity* **34**, 015001 (2016).
- [30] H. Fan, D. He, and S. Feng, Experimental study of a phase-sensitive heterodyne detector, *J. Opt. Soc. Am. B* **32**, 2172 (2015).
- [31] H. Vahlbruch, S. Chelkowski, K. Danzmann, and R. Schnabel, Quantum engineering of squeezed states for quantum communication and metrology, *New Journal of Physics* **9**, 371 (2007).
- [32] S. S. Y. Chua, S. Dwyer, L. Barsotti, D. Sigg, R. M. S. Schofield, V. V. Frolov, K. Kawabe, M. Evans, G. D. Meadors, M. Factourovich, R. Gustafson, N. Smith-Lefebvre, C. Vorvick, M. Landry, A. Khalaidovski, M. S. Stefiszky, C. M. Mow-Lowry, B. C. Buchler, D. A. Shaddock, P. K. Lam, R. Schnabel, N. Mavalvala, and D. E. McClelland, Impact of backscattered light in a squeezing-enhanced interferometric gravitational-wave detector, *Classical and Quantum Gravity* **31**, 035017 (2014).
- [33] W. P. Bowen, R. Schnabel, N. Treps, H.-A. Bachor, and P. K. Lam, Recovery of continuous wave squeezing at low frequencies, *Journal of Optics B: Quantum and Semiclassical Optics* **4**, 421 (2002).
- [34] K. McKenzie, E. E. Mikhailov, K. Goda, P. K. Lam, N. Grosse, M. B. Gray, N. Mavalvala, and D. E. McClelland, Quantum noise locking, *Journal of Optics B: Quantum and Semiclassical Optics* **7**, S421 (2005).
- [35] H. Vahlbruch, S. Chelkowski, B. Hage, A. Franzen, K. Danzmann, and R. Schnabel, Squeezed-field injection for gravitational wave interferometers, *Classical and Quantum Gravity* **23**, S251 (2006).
- [36] R. Schnabel, J. Harms, K. A. Strain, and K. Danzmann, Squeezed light for the interferometric detection of high-frequency gravitational waves, *Classical and Quantum Gravity* **21**, S1045 (2004).
- [37] K. McKenzie, N. Grosse, W. P. Bowen, S. E. Whitcomb, M. B. Gray, D. E. McClelland, and P. K. Lam, Squeezing in the audio gravitational-wave detection band, *Phys. Rev. Lett.* **93**, 161105 (2004).
- [38] R. Schnabel, Squeezed states of light and their applications in laser interferometers, *Physics Reports* **684**, 1 (2017).
- [39] S. Chelkowski, H. Vahlbruch, B. Hage, A. Franzen, N. Lastzka, K. Danzmann, and R. Schnabel, Experimental characterization of frequency-dependent squeezed light, *Phys. Rev. A* **71**, 013806 (2005).
- [40] K. McKenzie, D. A. Shaddock, D. E. McClelland, B. C. Buchler, and P. K. Lam, Experimental demonstration of a squeezing-enhanced power-recycled michelson interferometer for gravitational wave detection, *Phys. Rev. Lett.* **88**, 231102 (2002).
- [41] H. Vahlbruch, S. Chelkowski, B. Hage, A. Franzen, K. Danzmann, and R. Schnabel, Coherent control of vacuum squeezing in the gravitational-wave detection band, *Phys. Rev. Lett.* **97**, 011101 (2006).
- [42] H. Vahlbruch, M. Mehmet, K. Danzmann, and R. Schnabel, Detection of 15 db squeezed states of light and their application for the absolute calibration of photoelectric quantum efficiency, *Phys. Rev. Lett.* **117**, 110801 (2016).
- [43] J. Abadie, B. P. Abbott, R. Abbott, T. D. Abbott, et al. (LIGO Scientific Collaboration), A gravitational wave observatory operating beyond the quantum shot-noise limit, *Nature Physics* **7**, 962 (2011).
- [44] J. Aasi, J. Abadie, B. P. Abbott, R. Abbott, T. D. Abbott, M. R. Abernathy, et al. (LIGO Scientific Collaboration), Enhanced sensitivity of the ligo gravitational wave detector by using squeezed states of light, *Nature Photonics* **7**, 613 (2013).
- [45] Z. Zhai and J. Gao, Low-frequency phase measurement with high-frequency squeezing, *Opt. Express* **20**, 18173 (2012).
- [46] W. Li, Y. Jin, X. Yu, and J. Zhang, Enhanced detection of a low-frequency signal by using broad squeezed light and a bichromatic local oscillator, *Phys. Rev. A* **96**, 023808 (2017).
- [47] C. M. Caves and B. L. Schumaker, New formalism for two-photon quantum optics. i. quadrature phases and squeezed states, *Phys. Rev. A* **31**, 3068 (1985).
- [48] B. L. Schumaker and C. M. Caves, New formalism for two-photon quantum optics. ii. mathematical foundation and compact notation, *Phys. Rev. A* **31**, 3093 (1985).
- [49] T. Zhang, D. Martynov, A. Freise, and H. Miao, Quantum squeezing schemes for heterodyne readout, *Phys. Rev. D* **101**, 124052 (2020).
- [50] J. Zhang, Einstein-Podolsky-Rosen sideband entanglement in broadband squeezed light, *Phys. Rev. A* **67**, 054302 (2003).
- [51] Y. Ma, H. Miao, B. H. Pang, M. Evans, C. Zhao, J. Harms, R. Schnabel, and Y. Chen, Proposal for gravitational-wave detection beyond the standard quantum limit through EPR entanglement, *Nature Physics* **13**, 776 EP (2017).
- [52] S. L. Danilishin, F. Y. Khalili, and H. Miao, Advanced quantum techniques for future gravitational-wave detectors, *Living Reviews in Relativity* **22**, 2 (2019).
- [53] J. Südbeck, S. Steinlechner, M. Korobko, and R. Schnabel, Demonstration of interferometer enhancement through einstein-podolsky-rosen entanglement, *Nature Photonics* **14**, 240 (2020).
- [54] L. Barsotti, L. McCuller, M. Evans, and P. Fritschel, The a+ design curve, *LIGO Document T1800042* (2018).
- [55] H. J. Kimble, Y. Levin, A. B. Matsko, K. S. Thorne, and S. P. Vyatchanin, Conversion of conventional gravitational-wave interferometers into quantum nondemolition interferometers by modifying their input and/or output optics, *Phys. Rev. D* **65**, 022002 (2001).
- [56] S. L. Danilishin and F. Y. Khalili, Quantum measurement theory in gravitational-wave detectors, *Living Reviews in Relativity* **15** (2012).
- [57] V. B. Braginsky, Y. I. Vorontsov, and K. S. Thorne, Quantum nondemolition measurements, *Science* **209**, 547 (1980).
- [58] Y. Chen, S. L. Danilishin, F. Y. Khalili, and H. Müller-Ebhardt, QND measurements for future gravitational-wave detectors, *General Relativity and Gravitation* **43**, 671 (2011).
- [59] C. Helstrom, Minimum mean-squared error of estimates in quantum statistics, *Physics Letters A* **25**, 101 (1967).
- [60] V. B. Braginsky, M. L. Gorodetsky, F. Y. Khalili, and K. S. Thorne, Energetic quantum limit in large-scale interferometers, *AIP Conference Proceedings* **523**, 180 (2000).
- [61] M. Tsang, H. M. Wiseman, and C. M. Caves, Fundamental quantum limit to waveform estimation, *Phys. Rev. Lett.* **106**, 090401 (2011).
- [62] H. Miao, R. X. Adhikari, Y. Ma, B. Pang, and Y. Chen,

Towards the fundamental quantum limit of linear mea-

surements of classical signals, [Phys. Rev. Lett. \*\*119\*\*, 050801 \(2017\)](#).